Available online at www.sciencedirect.com

ScienceDirect

journal homepage: http://www.elsevier.com/locate/acme

Original Research Article

Prediction of formability of adhesive bonded steel sheets and experimental validation

Satheeshkumar V, Ganesh Narayanan R *

Department of Mechanical Engineering, IIT Guwahati, Guwahati 781 039, India

ARTICLE INFO

Article history:
Received 19 May 2014
Accepted 6 September 2014
Available online 7 October 2014

Keywords:
Adhesive bonded sheet
Tensile behaviour
Plane-strain
Limit strain
Prediction

ABSTRACT

The main aim of the present work is to predict the formability of adhesive bonded sheets and validate the same with experimental results at different adhesive properties. The tensile and in-plane plane-strain formability tests are carried out to predict the formability of adhesive bonded sheets. The forming limit strains are predicted using thickness gradient necking criterion (TGNC) and effective strain rate criterion (ESRC), and validated with the experimental limit strains. A simulation methodology has been analyzed thoroughly in the present work, and the prediction accuracies are compared and discussed.

The results show that the adhesive bonded blanks show improved elongation and forming limit strains as compared to un-bonded base materials with increase in hardener/resin ratio of adhesive. The true stress–strain predictions are accurate as compared to experimental data. There is a moderate difference in adhesive bonded sheets limit strains between predictions and experiments. This may be due to the absence of interface bonding between adhesive and base materials during predictions. The necking criterion, TGNC, shows better prediction as compared to ESRC.

1. Introduction

Adhesive bonding is one of the efficient structural component joining techniques in which an intermediate adhesive layer is used to bond substrates of different materials. Adhesive bonded sheets fabricated by this technique are utilized in the structural applications. Basic studies on the adhesive systems have been carried out to investigate the influence of different hardener/resin ratios and filler materials in the epoxy adhesive system. d'Almeida and Monteiro [1] investigated the influence of different resin/hardener ratios of the epoxy monomer, diglycidyl ether of bisphenol-A (DGEBA), with an aliphatic amine, triethylene tetramine (TETA) on mechanical properties by compression test. The results showed that the epoxy rich systems showed brittle behaviour which is associated with the development of a rigid macromolecular structure and the hardener rich systems showed fracture behaviour with a large deformation.

In the modelling of adhesive bonded blanks, Crocombo [2] stated that the term global yielding, which applies when a path of adhesive along the overlap region reaches the state in which it can sustain no further significant increase in applied load. It was found that global yielding gives accurate joint strengths

* *Corresponding author*. Tel.: +91 361 2582669.
E-mail addresses: ganu@iitg.ernet.in, rganesh.narayanan@yahoo.co.in (Ganesh Narayanan R.).
http://dx.doi.org/10.1016/j.acme.2014.09.002

during prediction. Kim et al. [3] introduced the superimposed finite element method for adhesive bonded joints to overcome difficulties in manual meshing technique. A cohesive zone model was used to model the interface between substrates and adhesive layer. It was found that the simulation of adhesive joints with the superimposed finite element method is efficient in view of the finite element discretization and shows accurate results.

The formability study on a two layer metallic sheet (Al1100/St12) bonded by polyurethane adhesive were performed by Aghchai et al. [4]. The two-layer sheet was assumed as an equivalent to a one-layer sheet by deriving equivalent mechanical parameters. In the other method, the mechanical properties of each layer were separately utilized to the two-layer sheet. It was observed that the two layer sheet improves the formability of a sheet which has low formability, but the influence of adhesive layer was not addressed. Morovvati et al. [5] investigated the influence of BHF on wrinkling of two-layer (aluminium-stainless steel) sheets bonded using polyurethane adhesive in the deep drawing process through an analytical method, FE simulations, and experiments. The results showed that the optimum BHF is dependent on the blank geometry, material properties and lay-up. It was observed that increase in blank holding force (BHF) decreases wrinkling in the deep drawing. Parsa et al. [6] carried out spring back evaluation of AA3105/polypropylene/AA3105 sandwich sheet materials after being subjected to double-curvature forming. Numerical simulation of double-curvature forming process was carried out using finite element programmes. It was found that the increase of tool radius in one direction not only decreased the spring back in that particular direction but also reduced the spring back in right angular direction.

Satheeshkumar and Ganesh Narayanan [7] investigated the influence of adhesive properties on the formability of adhesive-bonded dissimilar steel sheets. It was postulated and demonstrated that the improvement in formability of adhesive bonded blanks is due to the increase in elongation or improved plastic deformation of adhesives with increase in hardener/resin ratio. Further, increase in aspect ratio of artificially generated adhesive defects defect reduces the ductility of adhesive layer and thereby decreases the formability of adhesive bonded blanks. It was highlighted that the aspect ratio of the finite adhesive defect influences significantly on the formability of adhesive bonded blanks [8].

Takiguchi and Yoshida [9] analyzed the plastic bending of adhesive-bonded sheet metals through V-bending experiments. The specific increase of shear strain, as well as of the punch load which related directly to the change of the die-sheet contact boundary conditions was analyzed. The condition of deforming sheet at the initial stage supported by two edges of die was so called 'air-bending condition'. It was recommended that the air-bending operation for adhesive-bonded sheet metals for suppressing the shear deformation of the adhesive layer to within an acceptable limit. Further, the same authors proposed a new technique of plastic bending of adhesive-bonded sheet metals. The effect of forming speed on the deformation characteristics of adhesively bonded aluminium sheets was analyzed through V-bending experiments and numerical simulations using a rate-dependent constitutive model of plasticity for the adhesive. It was found that the large shear deformation and the geometrical imperfection caused by large transverse shear deformation occurring in the adhesive layer are suppressed by high-speed forming since the deformation resistance becomes higher at high strain rate [10].

From the above discussion, it is understood that the adhesive properties influence significantly the mechanical properties of the adhesive bonded blanks. The studies on the formability of bonded sheets have been addressed to a lesser extent. Most of the present studies are based on the delamination behaviour, strength requirement and rheological analysis. The main objective of the present work is to predict the forming behaviour of adhesive bonded sheets, namely tensile behaviour and in-plane plane strain (IPPS) formability, at different adhesive properties. Since adhesive bonded blanks are being used in almost all manufacturing sectors, this study will be helpful to sort out quickly the decisions by conducting similar virtual experiments. The mechanical properties of adhesives obtained from tensile tests are utilized for predicting the forming behaviour of adhesive bonded blanks without considering interfacial bonding between adhesive and base materials. The limit strains of adhesive bonded blanks are evaluated by using thickness gradient based necking criterion (TGNC) and effective strain based necking criterion (ESRC) which are used for predicting limit strains of unbonded sheet metals. These two necking criteria are used to check the applicability of predicting the limit strains in adhesive bonded blanks. Finally, the predicted results are validated with experimental data.

2. Methodology

In this section, the materials used in the experiments and the method of determining mechanical properties of epoxy adhesive, DDQ steel and SS 316L sheet metals are discussed. The method of evaluating the forming behaviour of adhesive bonded blanks through experiment is described. The representation of adhesive bonded blanks to predict their formability is illustrated. The formulation for predicting the true stress–strain behaviour of adhesive bonded sheets, and the necking criteria used for predicting the limit strains in base materials constituting adhesive bonded blanks are also presented.

2.1. *Experimental materials and mechanical properties*

Two dissimilar materials namely deep drawing quality (DDQ) cold rolled steel ($C\%$ = 0.100, $Si\%$ = 0.12 and $Mn\%$ = 0.600) and stainless steel (SS316L) ($C\%$ = 0.016, $Si\%$ = 0.335, $Mn\%$ = 1.209, $Cr\%$ = 16.413, $Ni\%$ = 10.222) sheets were used as base materials in the fabrication of adhesive bonded blanks. The thickness of base materials is 0.6 mm each. The base materials were tested as per ASTM E646-98 standard and the mechanical properties are tabulated in Table 1. The plastic strain ratio (R) was evaluated as per ASTM-E517 standard. The adhesive system used in this study was commercially available Bisphenol-A-Epicholorhydrin type epoxy resin (Part A) and Polyamidoamine type hardener (Part B). The adhesive properties are varied by changing the hardener/resin ratio. The stoichiometric ratio of hardener/resin ratio of epoxy adhesive system is 0.8:1.

Table 1 – Mechanical properties of DDQ steel and SS 316L sheets.

Materials	Young's modulus (GPa)	Yield strength (MPa)	Ultimate tensile strength (MPa)	Elongation [%] at failure in 50 mm gauge length	Strain hardening coefficient (n)	Strength coefficient K (MPa)	Plastic strain ratio		
							R_0	R_{45}	R_{90}
DDQ steel	210	189 ± 5	352 ± 5	39 ± 2	0.245 ± 0.005	620 ± 25	1.32	1.13	1.58
SS 316L	200	250 ± 5	610 ± 15	59 ± 2	0.466 ± 0.013	1352 ± 25	1.37	1.54	1.66

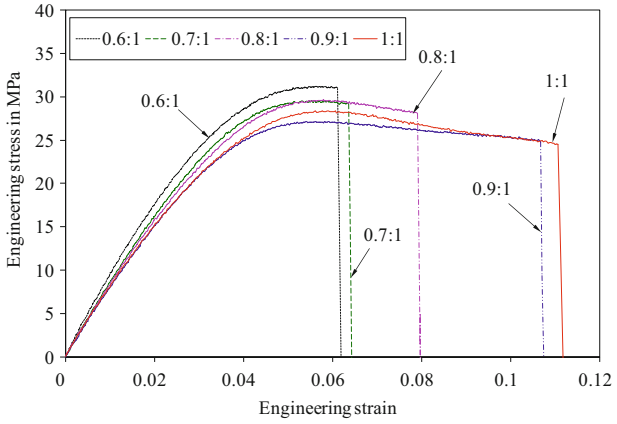

Fig. 1 – Comparison of engineering stress–strain behaviour of adhesive samples with different hardener/resin ratios.

The adhesive samples with different hardener/resin ratios were prepared by using appropriate moulds and tested as per ASTM D 638-I standard. Fig. 1 shows the engineering stress–strain behaviour of adhesive samples with different hardener/resin ratios. It is noticed that the increase in hardener/resin ratio increases the elongation the epoxy adhesive specimens. About 6.5% elongation is observed for the epoxy adhesive specimen with the hardener/resin ratio of 0.6:1 and about 11.2% elongation is observed with hardener/resin ratio of 1:1. A large deformation is observed for the epoxy adhesive specimen with hardener/resin ratio of 1:1. This is due to the excess amount of hardener molecules not finding enough resin molecules to accomplish cross-links. The non-reacted amine groups turn the specimen into plastic in nature. But in the case of hardener/resin ratio of 0.6:1, relative excess of resin monomer would not find enough hardener molecules which turns the adhesive specimen into brittle and causes the low deformation capacity. The epoxy adhesive specimens with resin rich formulation would then behave as soft spots like voids in its polymeric structure from where cracks may be originated [2,9]. Table 2 shows the mechanical properties of epoxy adhesive with different hardener/resin ratios determined from Fig. 1. The density of adhesive with different hardener/resin ratios were measured as per ASTM D1505 standard. The density was measured through density metre using cubic shaped adhesive samples with different hardener/resin ratios as per standard procedure.

2.2. *Experimental evaluation of forming of adhesive bonded blanks*

The adhesive bonded tensile specimens were prepared according to ASTM E646-98 standard by using epoxy adhesive system with different levels of hardener/resin ratio (by weight) like 0.6:1, 0.7:1, 0.8:1, 0.9:1, 1:1 with reference to the stoichiometric ratio. The homogeneous mixture of epoxy adhesive with different hardener/resin ratios was casted on the base materials surface smoothly with the help of a fabricated setup. The uniform adhesive thickness was maintained by using appropriate mould. After curing of adhesive bonded specimens, the average thickness of adhesive layers in adhesive bonded blanks was found to be 1 ± 0.015 mm. In the present study, the influence of hardener/resin ratio on the forming of adhesive bonded blanks were also analyzed through in-plane plane-strain (IPPS) formability tests. The main focus of this specific investigation is to study the critical forming limit of adhesive bonded blanks at the plane-strain condition. About 150 formability tests were simulated with different dimensions and geometries and strain paths were predicted using finite element simulations. The optimized geometry of IPPS specimen was used for fabricating adhesive bonded IPPS samples (Fig. 2a). The average thickness of adhesives in adhesive bonded blanks was found to be 1 ± 0.013 mm.

All the tests on adhesive bonded specimens were carried out in the INSTRON machine with a cross-head speed of 1 mm/min

Table 2 – Properties of epoxy adhesive.

H/R ratio	Young's modulus (GPa)	Ultimate tensile strength (MPa)	Uniform elongation (%)	Total elongation (%) (at 57 mm gauge length)	Density × 10^{-7} (kg/mm^3)
0.6:1	0.995 ± 0.0055	34 ± 3	5.508 ± 0.1	6 ± 0.1	7.85
0.7:1	0.872 ± 0.0055	30 ± 0.5	5.596 ± 0.05	6 ± 0.2	7.85
0.8:1	0.867 ± 0.0055	30 ± 0.5	5.705 ± 0.03	8 ± 0.5	7.78
0.9:1	0.840 ± 0.0055	28 ± 0.2	5.720 ± 0.29	10.5 ± 0.25	7.7
1:1	0.839 ± 0.019	28 ± 0.5	6.093 ± 0.2	11 ± 1.5	7.76

Note: H/R ratio – hardener per resin ratio.

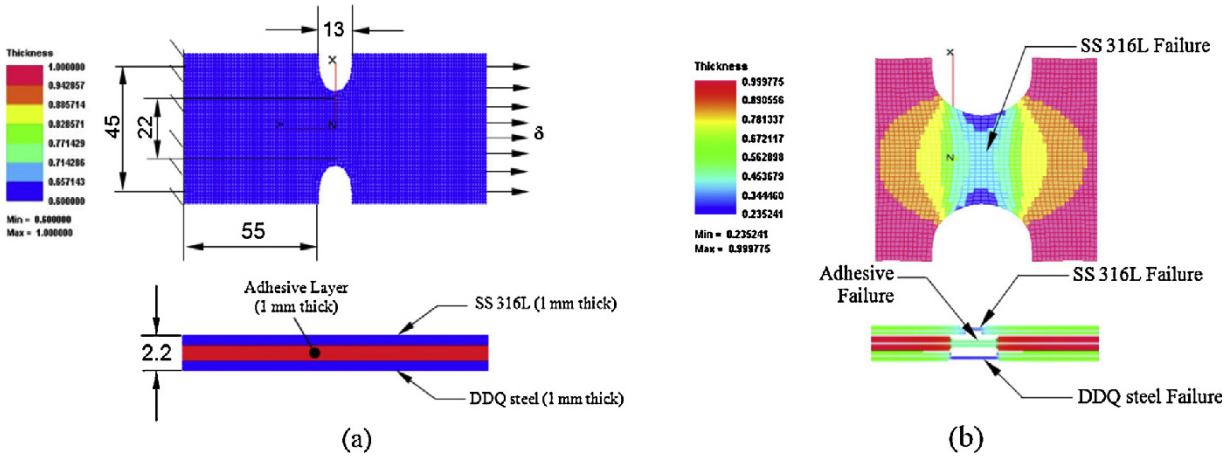

Fig. 2 – Boundary conditions of IPPS adhesive bonded blank in the simulation: (a) Before failure and (b) After failure.

at room temperature. After the test completion, the load–extension behaviour of all bonded blanks was obtained from the machine data and converted into engineering stress–strain behaviour and true stress–strain behaviour. Further, the limit strains were evaluated by measuring the length of major and minor axes of the deformed circular grids at the failure region of the tested blanks by using profile projector. The limit strains were measured in both base materials constituting adhesive bonded blanks. The average initial diameter of circular grids was calculated as 2.8 ± 0.05 mm. Three specimens were tested in each case to check the repeatability, and if the repeatability is not good, fourth test was performed.

2.3. *Predicting the forming behaviour of adhesive bonded blanks*

The finite element (FE) simulation was carried out using a commercially available elasto-plastic explicit dynamic FE code. The CAD models of tensile and IPPS specimens were meshed using the facility available in the code. The meshing was done with quadrilateral shell elements of the Belytschko–Tsay formulation. The average mesh size of about 2 mm was used throughout the tensile specimen and 1 mm was used for IPPS specimen, as there is a notch region in the IPPS sample.

In order to generate adhesive bonded blanks for FE simulations, three similar specimens were generated on the same plane and positioned one above other as shown in Figs. 2a and 3a without considering any bonding conditions. The top and bottom layers are base materials (DDQ steel and SS 316L), and the centre layer is adhesive. The base materials properties of DDQ steel and SS 316L given in Table 1 were incorporated during FE simulations. The total number of elements was about 805 in tensile test and about 15,174 in IPPS formability test. Hollomon's power law ($\sigma = K\varepsilon^n$; where, K - strength coefficient and n – strain-hardening exponent) was used to describe the strain-hardening behaviour of base materials. Hill's 1948 isotropic hardening yield criterion [11] was used as the plasticity model for DDQ steel and SS 316L materials. The adhesive stress–strain behaviour was obtained from experiments (Fig. 1). Figs. 2b and 3b show the failed samples of adhesive bonded blanks respectively from tensile and IPPS forming tests during simulations. The data was converted into true stress–strain behaviour by following standard procedure. The adhesive layer positioned between base materials was considered as an isotropic material. The true stress–strain behaviour and forming limit strains were predicted from FE simulations of tensile and IPPS forming tests. The limit strains are predicted using ESRC and TGNC (described later), and validated with experimental results.

2.4. *Prediction of stress–strain behaviour of adhesive bonded sheets*

Fig. 4a–c shows the schematic of failure pattern and load sharing during tensile and IPPS formability testing of adhesive

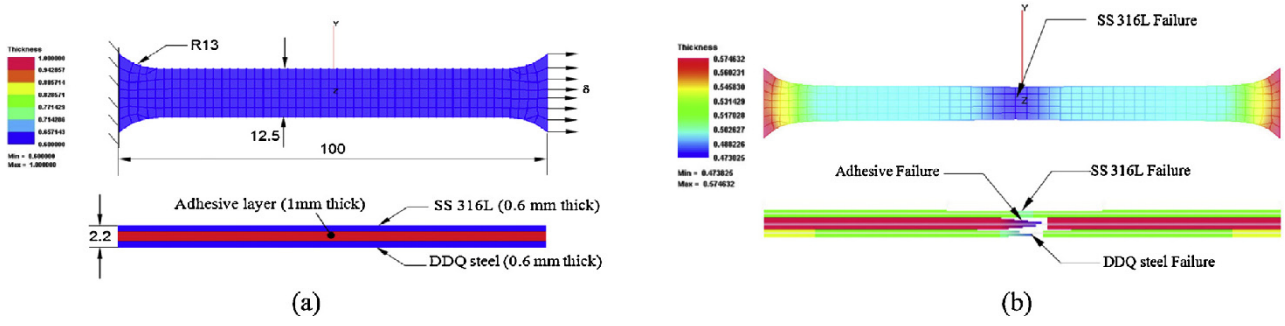

Fig. 3 – Boundary conditions of tensile adhesive bonded blank in the simulation: (a) Before failure and (b) After failure.

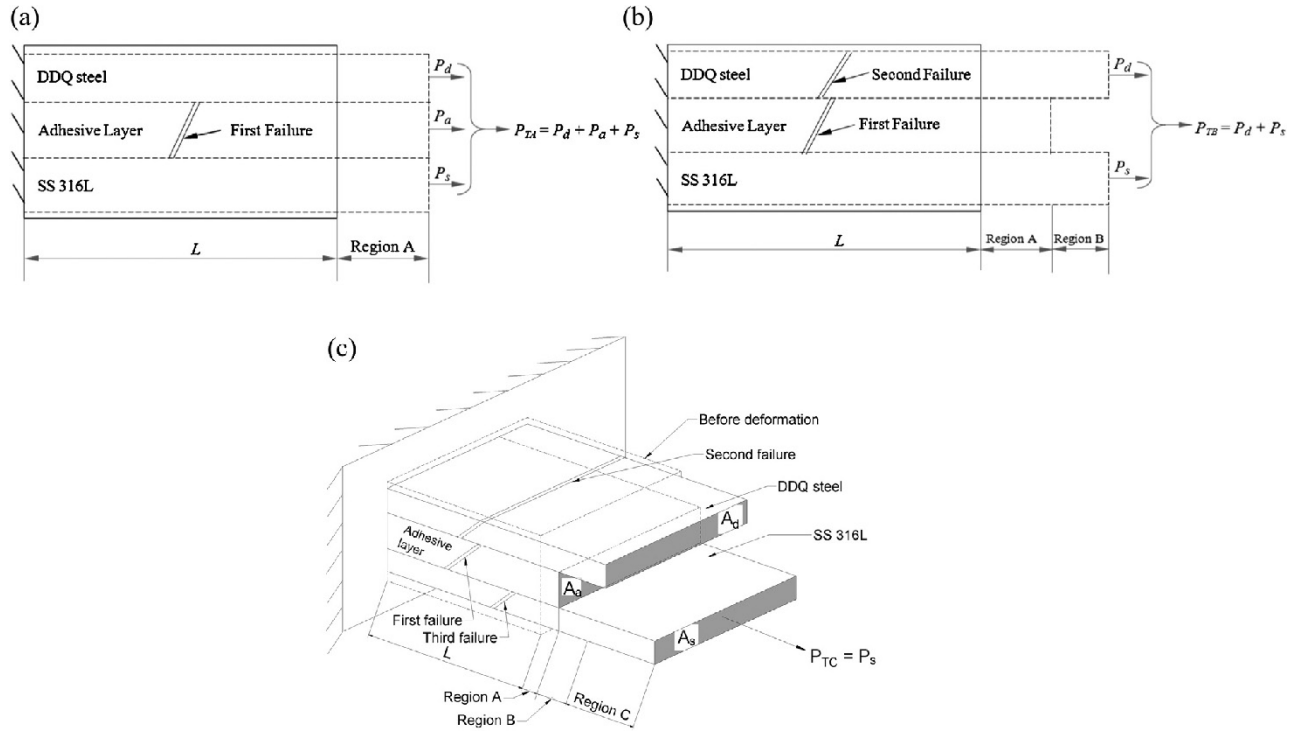

Fig. 4 – Schematic of load sharing in adhesive bonded blank during tensile test showing different deforming regions (Regions A, B and C) (where P_{TA}, P_{TB} and P_{TC} – total load in regions A, B and C, respectively).

bonded blanks. The deformation of adhesive bonded blanks is designated by different regions such as region A, B and C in the true stress–strain behaviour. The global deformation of adhesive layer, DDQ steel and SS 316L is designated as region A, the deformation of DDQ steel sheet and SS 316L sheet is termed as region B and the deformation of SS 316L only is termed as region C. Since the base materials and adhesive layer constituting in the adhesive bonded blank hold their individual mechanical properties during simulation, the true stress is calculated by the governing Eqs. (3–5) in regions A–C, respectively. The above observations are made from many experimental results.

Let, total load, P_T

$$P_T = P_d + P_a + P_s \tag{1}$$

where P_d – load on DDQ steel sheet in adhesive bonded blank; P_a – load on adhesive layer in adhesive bonded blank; P_s – load on SS 316L sheet in adhesive bonded blank.

$$P_T = \sigma_a A_a + \sigma_d A_d + \sigma_s A_s \tag{2}$$

where σ_a, σ_d and σ_s - respectively true stress of adhesive layer, DDQ steel and SS 316L sheets. A_a, A_d and A_s - respectively instantaneous area of adhesive layer, DDQ steel and SS 316L. In region A, the total load is shared by all three layers (DDQ steel, adhesive and SS 316L) which are deformed together till failure of adhesive layer as shown in Fig. 4a and the total true stress (σ_A) is calculated by Eq. (3).

$$\text{Region A} \rightarrow \sigma_A = (\sigma_a A_a + \sigma_d A_d + \sigma_s A_s)/A_{T1} \tag{3}$$

where σ_A – overall true stress in region A, A_{T1} – total instantaneous area in region A. Similarly, in region B, the total load is shared by base materials only (DDQ steel and SS 316L) as the adhesive has failed, and they deform together till failure of DDQ steel sheet as shown in Fig. 4b and Eq. (4) is followed for σ–ε evaluation.

$$\text{Region B} \rightarrow \sigma_B = (\sigma_d A_d + \sigma_s A_s)/A_{T2} \tag{4}$$

where σ_B – overall true stress in region B, A_{T2} – total instantaneous area in region B. In region C, the load is taken by SS 316L only which fails at last as shown in Fig. 4c and total stress (σ_C) is given by Eq. (5)

$$\text{Region C} \rightarrow \sigma_C = \sigma_s A_s / A_{T3} \tag{5}$$

where A_{T2} – total instantaneous area in region C which is equal to A_s.

2.5. *Prediction of limit strains of adhesive bonded sheets: necking criteria*

The flow localization of sheet forming occurs subsequent to uniform deformation and limits formability. The flow localization is generally characterized by a necking phenomenon and finally failure occurs when the critical limit strains are attained. Narasimhan and Wagoner [12] predicted forming limit diagrams of thin sheets based on two-dimensional finite thickness defects. It is seen from this analysis that the absolute location of FLC depends not only on material properties, but also on the choice of failure criterion, defect geometry, and details of simulative model mainly like mesh size, number of defect dimensions. Sujit et al. [13] developed a new failure criterion termed by thickness gradients that

develop during biaxial stretching. This new criterion can be used under a wide range of forming conditions to predict limit strains. The developed criterion predicts less dependence of limit strains on the degree of biaxiality for the range of material properties investigated.

2.6. *Effective strain rate based criterion (ESRC)*

ESRC is defined as the ratio of effective strain rate in the neck to that in the safe region (or bulk), and is written as [12]

$$\begin{aligned} ESRC = {} & \text{Effective strainrate in the neck region}/ \\ & \text{Effective strainrate in the safe region} \\ & \geq 4 \Rightarrow \text{material failure necking} \end{aligned} \quad (6)$$

The ratio 4 is a 'lower bound value' below which limit strains are not reached, and the strain rate ratio increase unstably once the criterion is reached, which is the indication for the occurrence of necking. The major strain and minor strain in the bulk element at which the criterion is satisfied indicate the limit strain in that strain path.

2.7. *Thickness gradient based necking criterion (TGNC)*

Generally, necking is understood as a localized thinning phenomenon and this criterion basically determines localized region within the deforming sheet where a thickness gradient develops. The necking occurs in the sheet metal when the thickness gradient falls below 0.92 and is also applied to predict the FLC [13]. In the present simulations, element pairs where the thickness ratio equals or falls below 0.92 are considered as necked elements. The major strains in all the thicker elements are noted. The largest major strain and the corresponding minor strain of such elements are treated as the forming limit strain. The thickness gradient necking criterion is given by Eq. (7),

$$\begin{aligned} TGNC = {} & \frac{\text{Thickness in necking element}}{\text{Thickness in bulk element}} \\ & = t_n/t_{n-1} \text{ or } t_n/t_{n+1} \\ & \leq 0.92 \Rightarrow \text{material failure necking} \end{aligned} \quad (7)$$

These ESRC and TGNC criteria have been applied for single metal sheets and also for welded sheets which are on the same plane. In the present work, the applicability of ESRC and TGNC criteria for adhesive bonded sheets will be checked and discussed. It is expected that the criteria are modified because of the presence of adhesive, and the original criteria are unsuitable for adhesive bonded blanks.

3. Results and discussion

In this section, the failure of adhesive bonded blanks with different hardener/resin ratios is compared between experiment and prediction. The tensile behaviour of adhesive bonded sheets is compared and analyzed between experiment and prediction. Further, the forming limit strains in base materials constituting adhesive bonded blanks with effect of hardener/resin ratio predicted by TGNC and ESRC are compared with experiment and discussed.

3.1. *Failure of adhesive bonded blanks at different hardener/resin ratios: experiment and prediction*

Fig. 5a and b shows the comparison of true stress–strain behaviour of DDQ steel and SS 316L between experimental and predicted results, respectively, from tensile test. For DDQ steel, there is about 7 MPa variation in true strain at failure and about 2.2% variation in true strain between experimental and predicted results. There is a good agreement between experimental and predicted results in the case of SS 316L. The base materials are modelled by Hollomon strain hardening equation and Hill's 1948 yield criterion.

Tables 3 and 4 compare the progression at failure of adhesive and base materials from experiments and FE simulations for varying hardener/resin ratios respectively during tensile test and IPPS formability tests. In simulation results, the failure stage of base materials are obtained from effective strain rate based necking criterion (ESRC) and thickness gradient-based necking criterion (TGNC). It is understood that whenever the failure criteria are satisfied, necking occurs in the base materials and that progression is noted as failure progression. The adhesive failure stage is determined from the load drop observed in the load-progression data from FE predictions. In the case of experiments, all

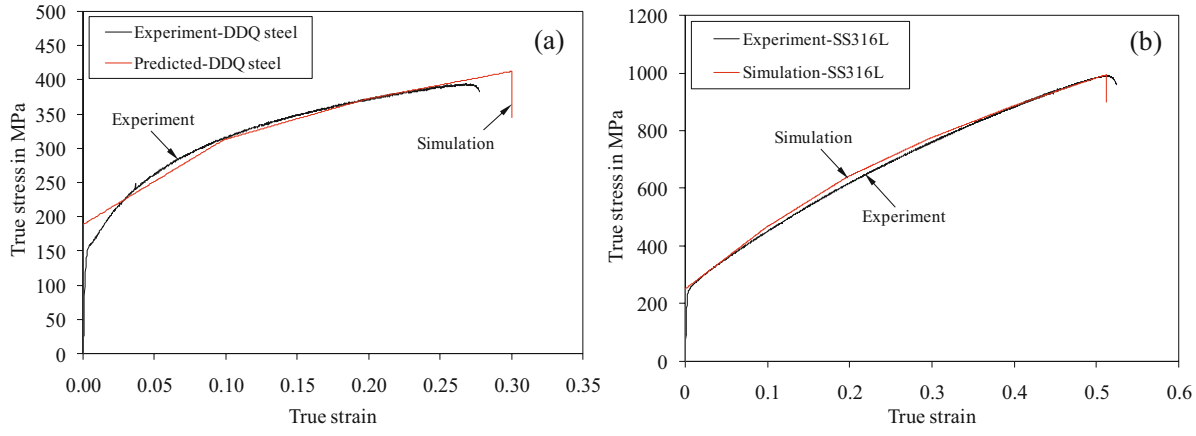

Fig. 5 – Comparison of true stress–strain behaviour of base materials between experimental and prediction: (a) DDQ steel and (b) SS 316L.

Table 3 – Prediction of progression at failure of adhesive bonded blanks with different *H/R* ratios in tensile test.

H/R ratio	Adhesive layer failure (mm)			DDQ steel sheet failure (mm)					SS316L sheet failure (mm)				
	Experiment	Simulation	Variation %	Experiment	Simulation				Experiment	Simulation			
					ESRC	Variation %	TGNC	Variation %		ESRC	Variation %	TGNC	Variation %
Single sheet	–	–	–	26.3	27.42	4.3	28.68	9.1	52.4	51.72	1.3	53.46	2.0
0.6:1	9.34	9.5	1.7	27.12	24.54	9.5	26.52	2.2	55.0	52.8	4.0	55.38	0.7
0.7:1	9.5	10.0	5.3	29.0	24.54	15.4	26.52	8.1	53.9	53.1	1.5	55.56	3.1
0.8:1	12.5	10.5	16.0	28.1	24.54	12.7	26.52	5.6	55.5	50.88	8.3	56.16	1.2
0.9:1	12.7	11.0	13.4	29.3	24.54	16.3	26.52	9.5	57.8	53.1	8.1	56.16	2.8
1:1	13.7	11.5	16.1	30.0	24.42	18.6	26.4	12.0	59.2	52.68	11.0	56.28	5.5

Table 4 – Prediction of progression at failure of adhesive bonded blanks with different *H/R* ratios in IPPS formability test.

H/R ratio	Adhesive layer failure (mm)			DDQ steel sheet failure (mm)					SS316L sheet failure (mm)				
	Experiment	Simulation	Variation %	Experiment	Simulation				Experiment	Simulation			
					ESRC	Variation %	TGNC	Variation %		ESRC	Variation %	TGNC	Variation %
Single sheet	–	–	–	4.7	5.88	25.1	5.94	26.4	8.6	15.8	83.7	15.88	84.7
0.6:1	1.1	5.02	78.1	5.1	6.46	26.7	6.56	28.6	8.6	16.76	94.9	16.58	92.8
0.8:1	1.3	5.50	76.4	5.3	6.46	21.9	6.56	23.4	9.6	16.76	74.6	16.58	72.7
1:1	2.4	6.12	60.8	5.6	6.46	15.4	6.56	17.1	11.8	16.76	42.0	16.58	40.5

the failure stages were obtained from the load drop of load-progression behaviour of tensile test. It is observed from the experimental results that the progression at failure of adhesive layer and base materials in adhesive bonded sheets increases with increase in hardener/resin ratio. In the simulation results, a similar trend of delay in failure is noticed only in the case of adhesive layer deformation, but not in the constituting base materials. In the case of predicted (simulation) results from Table 3, it is observed that with increase in hardener/resin ratio, the progression at failure of adhesive increases from 9.5 mm to 11.5 mm. Similar results are seen in the case of IPPS formability tests, that is from 5.02 mm to 6.12 mm (Table 4). In the case of tensile test (Table 3), there exists moderate agreement between the experimental and predicted results. In the case of IPPS forming tests, the predictions are considerably different. The influence of hardener/resin ratios on base materials failure is not predicted properly during simulation results, unlike in experiments. The progression at failure of constituting base materials is almost constant during predictions. This implies that the accuracy of predictions decreases with increase in hardener/resin ratio in the case of tensile test and vice versa in the case of IPPS forming test.

Among the two failure criteria, TGNC predicts the failure stage later than ESRC in most of the cases of tensile and IPPS forming tests. In other words, TGNC is accurate than ESRC in predicting the constituting base material failure in the case of tensile test, while both perform equally, not accurately in the case of IPPS forming test. With respect to adhesive bonded blanks, there is about 4–18.6% variation between experiment and ESRC prediction, and about 0.7–12% variation between experiment and TGNC prediction in the case of tensile test.

In the case of prediction through FE simulations, the effect of adhesive properties is not captured and hence the progression at failure of base materials remains same in all the cases. This is believed to happen mainly because of absence of adhesive bonding (or adhesion) during FE simulations. So, the change in mechanical behaviour of adhesive bonded sheets is not only because of change of adhesive properties, but also due to adhesion methods and properties. There is a poor agreement between experiment and predicted progression at failure in the case of IPPS forming test which is unexpected. This is believed to happen because of the presence of notch, changing the behaviour of whole adhesive bonded sheets during prediction. Moreover, this sample deforms near plane-strain conditions, which is the critical strain path in sheet deformation.

3.2. *Experimental evaluation and prediction of tensile behaviour of adhesive bonded sheets*

Fig. 6a and b shows the overall comparison of tensile (true stress–strain) behaviour of adhesive bonded blanks with different hardener/resin ratios obtained from experiments

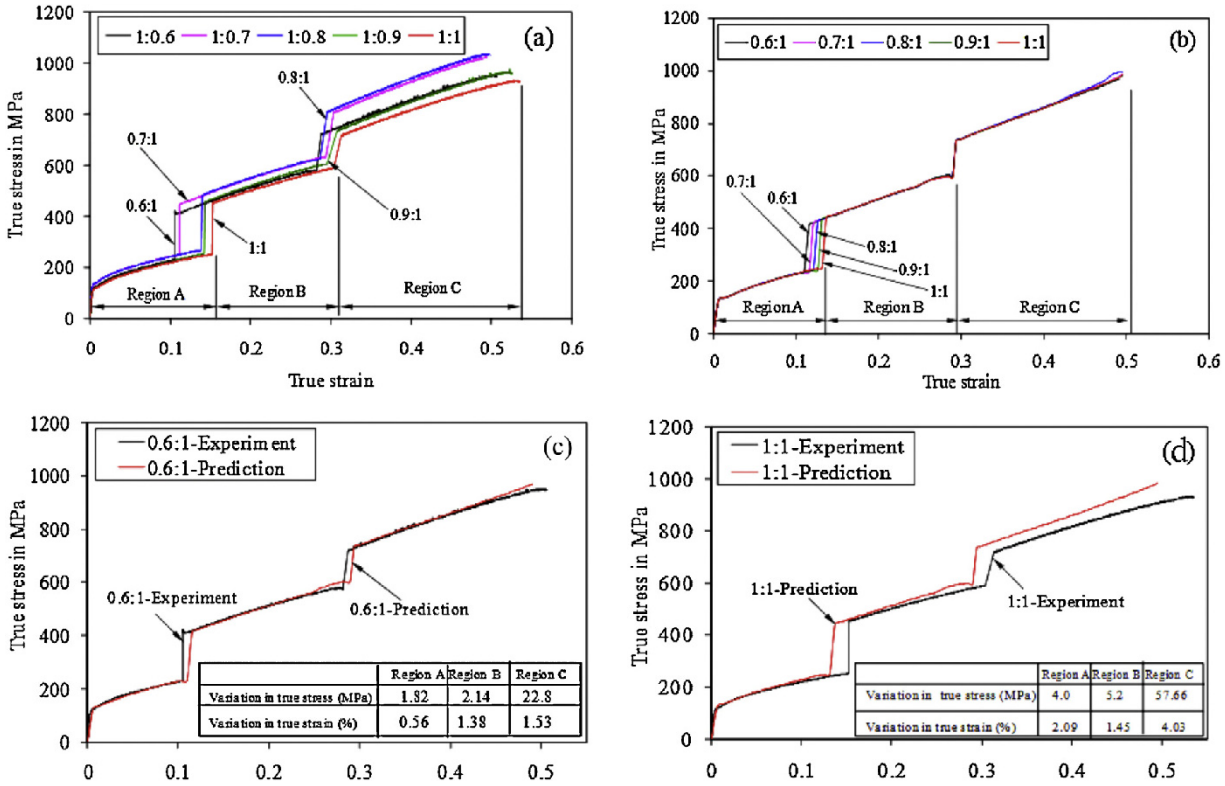

Fig. 6 – Comparison of tensile (true stress–strain) behaviour of adhesive bonded blanks with different hardener/resin ratios: (a) Experiments (variation in ultimate tensile strength = ±8 MPa, and in elongation at failure = ±1%), (b) Simulations, (c) *H/R* = 0.6:1, (d) *H/R* = 1:1 (where Region A → tensile behaviour of adhesive layer, DDQ steel sheet and SS316L sheet, Region B → tensile behaviour of DDQ steel sheet and SS316L sheet of adhesive bonded blank, Region C → tensile behaviour of SS 316L sheet of adhesive bonded blank).

and FE simulations, respectively. Fig. 6c and d shows the individual comparison of tensile (true stress–strain) behaviour of adhesive bonded blanks with different hardener/resin ratios obtained from experiments and predictions. While evaluating the tensile (true stress–strain) behaviour of adhesive bonded blanks from the load-progression experimental data, the deformation of all three layers constituting adhesive bonded blanks (adhesive layer, DDQ steel and SS 316L) was taken into account and true stress–strain was calculated in region A through Eq. (3). After failure of adhesive layer, the deformation of DDQ steel and SS 316L sheets was taken into account for calculating true stress–strain in region B through Eq. (4). Similarly, after failure of DDQ steel sheet, Eq. (5) was used in region C to evaluate σ–ε behaviour. It is observed from experimental results that the true strain at failure increases with increase in hardener/resin ratio in all the regions A, B and C (Fig. 6a). It is due to improved plasticity of adhesive layer which hold rich in hardener formulation in the adhesive system [7]. While comparing experimental and predicted results (Fig. 6c and d), the global tensile behaviour of adhesive bonded blanks follows the same trend till adhesive failure that is with increase in hardener/resin ratio, the true strain at failure of adhesive (region A) increases. This is true in the case of experiment and simulation results. But it does not occur in regions B and C.

In the prediction of true stress–strain behaviour of (Fig. 6b), the adhesive layer that is governed by its mechanical properties shows improvement in ductility in region A. But there is no influence of adhesive layer on ductility of base materials constituting adhesive bonded blanks as compared to the tensile (true stress–strain) behaviour obtained from experiments (Fig. 6a). From these results, it is believed that the ductility of adhesive bonded blanks is not only influenced by the plasticity of adhesive, but also its interfacial bonding (adhesive bonding) between base materials. There is about 0.42–2.09%, 0.45–1.45% and 0–4.03% variation respectively in true strain in regions A, B and C. Almost there is a good agreement in true stress between experimental and predicted results in all three regions except a few. On the whole, though the improvement in ductility of base materials constituting adhesive bonded blanks is not predicted accurately, the overall tensile behaviour prediction is encouraging.

Fig. 7a and b shows the comparison of % elongation (true strain) of regions A, B and C with different hardener/resin ratios between experiment and predicted results respectively from tensile and IPPS forming tests. Here the elongation % is obtained using the failure criteria (TGNC and ESRC).

The elongation increases with increase in hardener/resin ratio till failure of adhesive layer (Region A). This is true in the case of experiments and simulations. But in regions B and C, though the difference between experiment and predicted elongation values is less (<2%), the trend of increased elongation with increase in hardener/resin ratio is not observed (Fig. 7a). The true stress–strain behaviour of adhesive bonded sheets during IPPS forming test was evaluated for all the cases. The elongation at failure for different hardener/resin ratios is depicted in Fig. 7b. There is an increasing trend of elongation % with increase in hardener/resin ratio, from experiments and prediction in region A. But it is not reflected during predictions in regions B and C as compared to the experiments. Also there is a considerable disagreement between experimental and predicted elongation data.

3.3. *Forming limit strain prediction of adhesive bonded blanks with effect of hardener/resin ratio*

Fig. 8a and b demonstrates the variation of effective strain rate ratio with true major strain in bulk in base materials in adhesive bonded blanks with different hardener/resin ratios during tensile and IPPS forming tests simulation. It is understood that the effective strain rate ratio increases unstably once the criterion is reached, which is the indication for the occurrence of necking. The corresponding major strain and minor strain in the bulk element indicate the limit strain in that strain path. It should be noted that the ratios shown in the figures are arbitrary numbers that are less than or equal

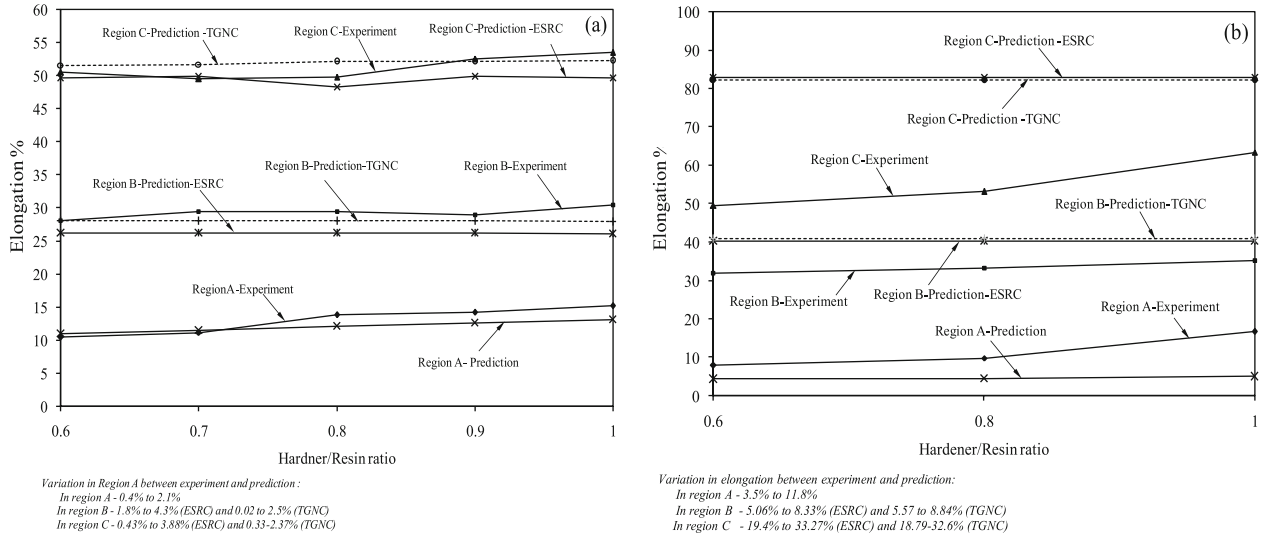

Fig. 7 – Comparison of percentage elongation (true strain) of adhesive bonded blanks with different hardener/resin ratios between experiment and predicted results: (a) Tensile test and (b) IPPS formability test.

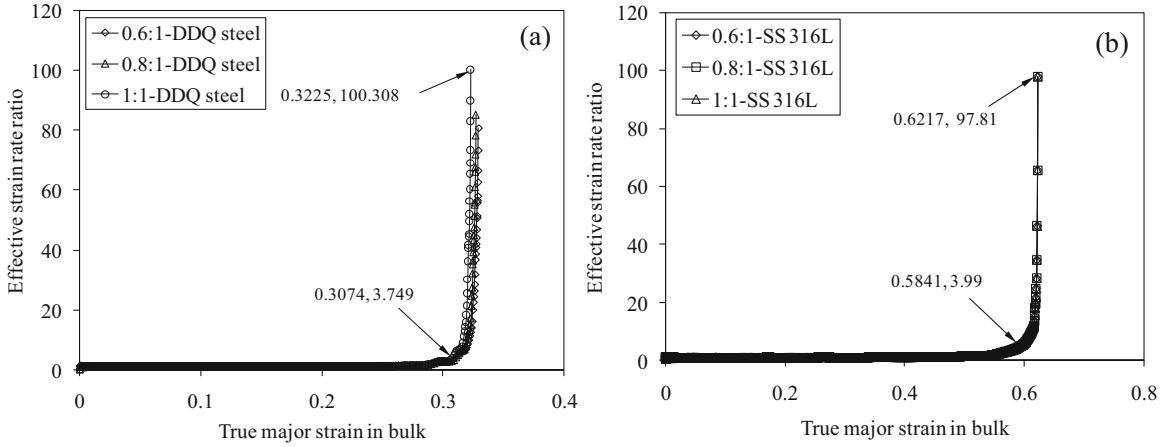

Fig. 8 – Variation of effective strain rate ratio with true major strain in bulk in base materials in adhesive bonded blanks with different *H*/*R* ratios: (a) DDQ steel (tensile test) and (b) SS 316L (IPPS forming test).

to ESRC above which a sudden increase in ratio is seen. It is observed that the ESRC defined for base materials that are unbonded is suitable for adhesive bonded sheets also. The true major strain in bulk saturates when the criterion is satisfied. Hence the criterion is not modified, and original criterion of ESRC ≥4 for failure to occur is used for prediction.

Fig. 9a and b shows the comparison of limit strains of DDQ steel and SS 316L base materials evaluated through experiment and prediction during tensile and IPPS forming tests, respectively. The limit strains of base materials are predicted by the necking criteria, ESRC and TGNC, and compared with experimental results. In tensile test (Fig. 9a), there is not much difference in major strain (<1.3%) between experiment and prediction by TGNC. About 4.2% and 6.3% difference in major strain is observed with DDQ steel and SS 316L, respectively, when the base materials are predicted by ESRC. A large difference (13.2–17.9%) in minor strain is observed between experiment and prediction by both TGNC and ESRC. While comparing limit strains obtained from IPPS forming test (Fig. 9b), a significant difference in both major and minor strain is noted between experimental and predicted (TGNC and ESRC) results. In the case of SS 316L, there is a slight variation in strain path from plane strain condition, as indicated by limit strain predicted through TGNC and ESRC. In general, the limits strains predicted by TGNC show less difference between experimental results than predicted by ESRC.

Fig. 10a and b presents the comparison of limit strain results in DDQ steel and SS 316L, respectively, in adhesive bonded blanks with different hardener/resin ratios obtained from experimental tensile test. It is observed that the true major and minor limit strain increase with increase in hardener/resin ratio in both DDQ steel and SS316L sheets. This signifies the improvement in limit strains and change in strain path.

Fig. 11a–f shows the comparison of limits strains in DDQ steel and SS 316L constituting adhesive bonded blanks with different hardener/resin ratios predicted by TGNC and ESRC from tensile and IPPS forming tests. The predicted results are compared with experimental results, and the variation in limit strains is also shown. It is observed that a considerable difference exists between experimental and predicted (by TGNC and ESRC) limit strain results. In tensile test, the true

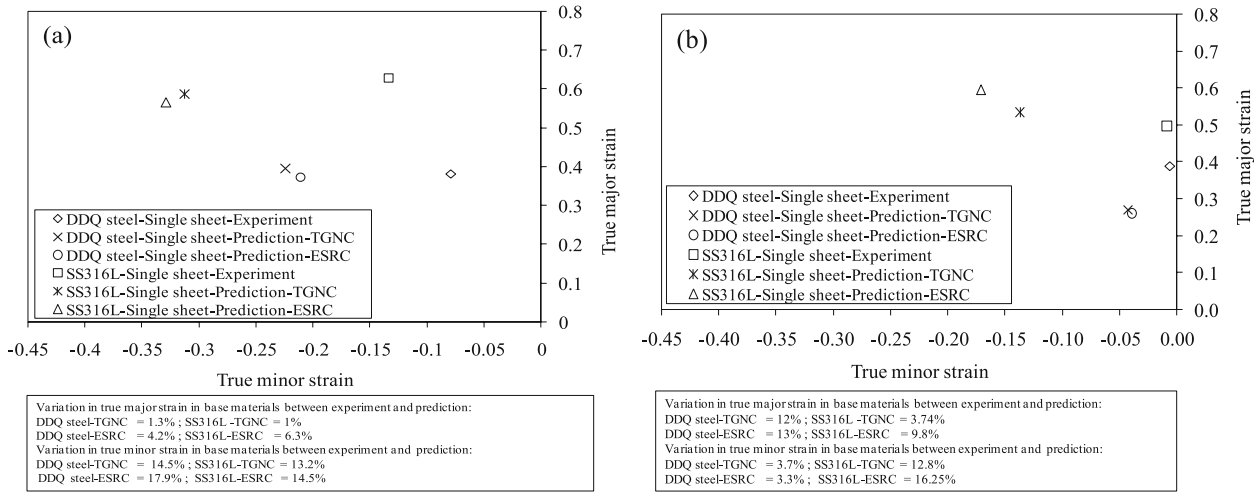

Fig. 9 – Comparison of experiment and prediction of base materials limit strain: (a) tensile test and (b) IPPS forming test.

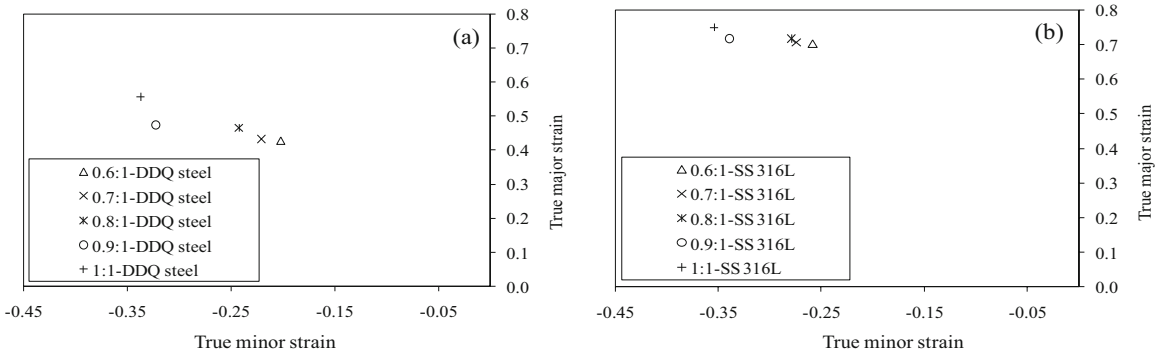

Fig. 10 – Comparison of experimental limit strain results of adhesive bonded blanks with different *H/R* ratio from tensile test: (a) DDQ steel and (b) SS 316L.

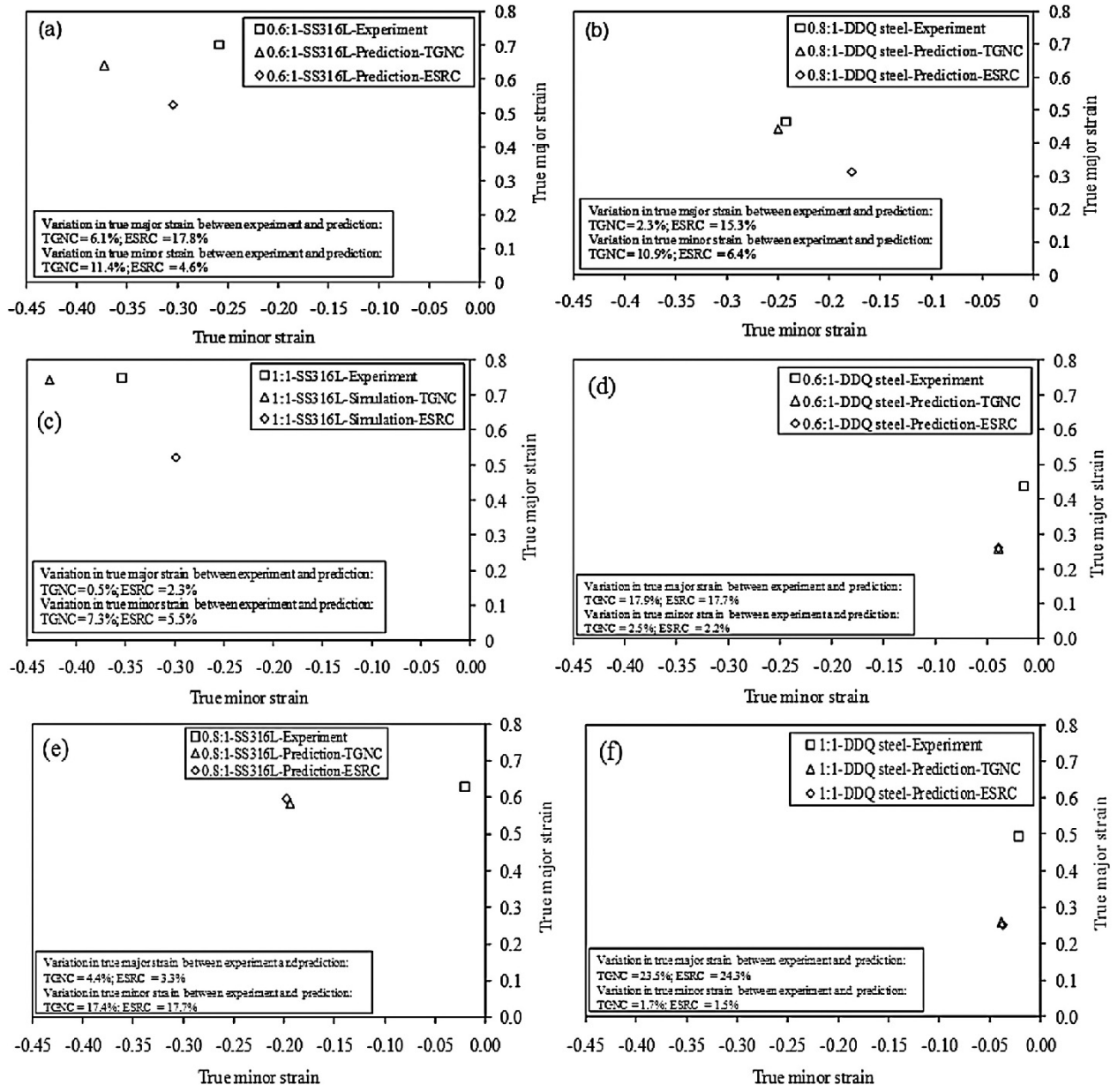

Fig. 11 – Comparison of limit strain results of adhesive bonded blanks with different *H/R* ratios between experiments and predictions: (a) *H/R* = 0.6:1-SS 316L (tensile test), (b) *H/R* = 0.8:1-DDQ steel (tensile test), (c) *H/R* = 1:1-SS 316L (tensile test), (d) *H/R* = 0.6:1-SS 316L (IPPS forming test), (e) *H/R* = 0.8:1-SS 316L (IPPS forming test), and (f) *H/R* = 1:1-DDQ steel (IPPS forming test).

major strain varies from 0.5% to 6% and the true minor strain varies from 7.3% to 11.5%, during TGNC predictions. While through ESRC predictions, the true major strain varies from 2.3% to 17.8% and the true minor strain varies from 4.6% to 6.4%. It is noted that the major strain predicted by TGNC show better agreement to the experimental results in most of the cases.

Similarly, in IPPS forming test, there is about 4.5–23.5% difference in true major strain and about 1.7–17.5% difference in true minor strain, during TGNC predictions. In the case of prediction by ESRC, there is about 3.3–24.3% difference in true major strain and about 2.2–17.7% difference in true minor strain. Though there is a large difference between experimental and predicted (by TGNC and ESRC) limit strain results, the predicted limit strain results are closer to each other.

In specific, during IPPS forming test, there exists a significant difference in the progression till failure of SS 316L between experimental and prediction results (Table 3). This large difference in progression is not reflected on the true major limit strains, but on the true minor strains of base materials predicted by TGNC and ESRC.

On the whole, though both the necking criteria, TGNC and ESRC are meant for base material (unbonded) formability prediction, the TGNC shows its superiority with less difference between experimental limit strain results in the present study. Since there is no interfacial bonding between adhesive and base materials, the base materials constituting adhesive bonded blanks behave as if like a single sheet. Further, the applicability of TGNC and ESRC will be checked for adhesive bonded blanks by considering interfacial bonding between adhesive and base materials.

4. Conclusions

From the present work, the following conclusions are drawn.

- The ductility of adhesive bonded blanks increases with increase in hardener/resin ratio till adhesive failure and this improvement in plasticity of adhesive layer increases the ductility of the base materials.
- There is a good agreement between experimental and predicted overall true stress–strain behaviour of adhesive bonded sheets. Though this is the case, the influence of changing adhesive properties on the tensile behaviour and IPPS formability is not predicted accurately.
- During forming limit strain prediction of adhesive bonded blank under the influence of hardener/resin ratio of the adhesive system, both ESRC and TGNC are applicable only to a moderate extent. On the whole, the predicted limit strain results based on TGNC shows better accuracy as compared to ESRC.
- Finally, in the present work, a simulation methodology has been analyzed thoroughly to predict the formability of adhesive bonded sheets. The inaccuracies in formability predictions are believed due to the absence of interface interaction between adhesive and base materials during simulation. Further investigation is required in this direction to improve the prediction accuracy.

REFERENCES

[1] J.R.M. d'Almeida, S.N. Monteiro, The effect of the resin/hardener ratio on the compressive behaviour of an epoxy system, Polymer Testing 15 (1996) 329–339.
[2] A.D. Crocombe, Global yielding as a failure criterion for bonded joints, International Journal of Adhesion and Adhesives 9 (3) (1989) 145–153.
[3] Y.T. Kim, M.J. Lee, B.C. Lee, Simulation of adhesive joints using the superimposed finite element method and a cohesive zone model, International Journal of Adhesion and Adhesives 31 (2011) 357–362.
[4] A.J. Aghchai, M. Shakeri, B. Mollaei-Dariani, Theoretical and experimental formability study of two-layer metallic sheet (Al1100/St12), Proceedings of the Institution of Mechanical Engineers, Part B: Journal of Engineering Manufacture 222 (2008) 1131–1138.
[5] M.R. Morovvati, B. Mollaei-Dariani, M.H. Asadian-Ardakani, A theoretical, numerical, and experimental investigation of plastic wrinkling of circular two-layer sheet metal in the deep drawing, Journal of Materials Processing Technology 210 (2010) 1738–1747.
[6] M.H. Parsa, S. Nasher al ahkami, M. Ettehad, Experimental and finite element study on the spring back of double curved aluminum/polypropylene/aluminum sandwich sheet, Materials and Design 31 (2010) 4174–4183.
[7] V. Satheeshkumar, R. Ganesh Narayanan, Investigation on the influence of adhesive properties on the formability of adhesive bonded steel sheets, Proceedings of the Institution of Mechanical Engineers, Part C: Journal of Mechanical Engineering Science 228 (3) (2014) 405–425.
[8] V. Satheeshkumar, R. Ganesh Narayanan, Formability of adhesive bonded steel sheets with artificial finite adhesive defects, Journal of Strain Analysis for Engineering Design 49 (5) (2014) 286–300.
[9] M. Takiguchi, F. Yoshida, Plastic bonding adhesive bonding of sheet metals, Journal of Materials Processing Technology 113 (2001) 743–748.
[10] M. Takiguchi, F. Yoshida, Analysis of plastic bending of adhesive-bonded sheet metals taking account of viscoplasticity of adhesive, Journal of Materials Processing Technology 140 (2003) 441–446.
[11] D. Banabic, Sheet Metal Forming Processes Constitutive Modeling and Numerical Simulation, Springer-Verlag, Heidelberg, 2010.
[12] K. Narasimhan, R.H. Wagoner, Finite element modeling simulation of in-plane forming limit diagrams of sheets containing finite defects, Metallurgical Transactions A 22 (11) (1991) 2655–2665.
[13] K. Sujit, P.P. Date, K. Narasimhan, A new criterion to predict necking failure under biaxial stretching, Journal of Materials Processing Technology 45 (1–4) (1994) 583–588.